THE RED CN BAND SYSTEM

By F. A. Jenkins, Department of Physics
University of California

Yale K. Roots, Department of Physics
Findlay College

and

Robert S. Mulliken, Ryerson Physical Laboratory
University of Chicago

(Received November 17, 1931)

Abstract

Rotational structure of red CN bands. The rotational structure of the (4,1), (5,2), (6,1), (6,2), (7,2), (7,3) and (8,3) bands of this system is measured on plates from the first order of a 21-foot grating. To excite the spectrum, carbon tetrachloride vapor was mixed with active nitrogen. The lines of each band are arranged in eight branches, giving a structure characteristic of a $^2\Pi \rightarrow {}^2\Sigma$ transition in which the spin doubling in $^2\Sigma$ is small. Missing lines show the $^2\Pi$ state to be inverted. Good agreement is obtained for the constants of the lower state with those of the violet CN system. The rotational constants of the $^2\Pi$ state are: $A=-52.2$ cm^{-1}, $B_v=1.6990-0.01746\ (v+\frac{1}{2})$ cm^{-1}, $D_v=-[6.133+0.0127\ (v+\frac{1}{2})]\times 10^{-6}$ cm^{-1}, $I_e=16.28\times 10^{-40}$ g cm^2, $r_e=1.236\times 10^{-8}$ cm. The $^2\Pi$ terms are represented accurately by the Hill and Van Vleck formula. Microphotometer measurements of photographic densities in the 8,3 band are given, and agree qualitatively with the theory. They show the $^2\Pi_{3/2}\rightarrow {}^2\Sigma$ band to be stronger than the $^2\Pi_{1/2}\rightarrow {}^2\Sigma$ band.

Spin doubling and Λ-doubling. A rough evaluation of the difference $F_1''(K)-F_2''(K)=\gamma_0\ (K+\frac{1}{2})$ is possible, and gives $\gamma_0=+0.0071$ and 0.0082 and for $v''=3$ and 2, respectively. For the states $v'=4$, 5 and 8, the Λ-doubling is regular, and of the form recently discussed by Mulliken and Christy. We find $p_0=0.00621$, 0.00853, 0.01872, $q_0=-0.000252$, -0.000365 and -0.000435 for $v'=4$, 5 and 8.

Perturbations. Three strong perturbations are found in $v'=6$, in T_{1c} at $J=13\frac{1}{2}$, in T_{1d} at $J=25\frac{1}{2}$ and in T_{2d} at $J=27\frac{1}{2}$. These are exactly as expected theoretically from the three corresponding perturbations found in the violet system by Rosenthal and Jenkins, and from an extrapolation of the unperturbed levels. An anomalous Λ-doubling in $^2\Pi_{1/2}{}^{(7)}$ is explained as a perturbation, with the difference that here the perturbing levels of $^2\Pi_{1/2}{}^{(7)}$ and $a^2\Sigma^{(12)}$ do not cross, but merely approach closely.

Vibrational structure. From measurements of the R_2 heads of 17 other bands, and correction to origins, the following expression is obtained for band origins:

$$\nu=11{,}043.20+1788.66\ (v'+\tfrac{1}{2})-12.883\ (v'+\tfrac{1}{2})^2-2068.79\ (v''+\tfrac{1}{2})+13.176\ (v''+\tfrac{1}{2})^2.$$

Perturbations of the band origins by 1 or 2 cm^{-1} occur for $v'=6$ and 7, and are evidently of similar origin to the rotational perturbations in these states. The vibrational numbering used here for the $^2\Pi$ state is that of Asundi and Ryde. This numbering, hitherto in doubt, has now been definitely established by a comparison of the observed vibrational intensity relations with those predicted by the wave mechanics with the method of Condon.

Introduction

THE extensive system of "cyanogen" bands which has its maximum intensity in the orange and red was first measured in vacuum-tube spectra of compounds containing carbon and nitrogen.[1] In the first studies of Ray-

[1] H. Kayser, "Handbuch der Spectroscopie," Vol. 7, pp. 135–7.

leigh[2] and of Rayleigh and Fowler[3] on the spectra excited by active nitrogen, it was discovered that carbon compounds produce a bright cyanogen spectrum exceptionally free from impurities. The intensity of the red CN system relative to the violet system varies greatly with the compound used. In particular, the halogen compounds, such as chloroform and carbon tetrachloride, were found to give the red system such predominance that the glow produced is orange, instead of the usual lilac color. Since the bands of the red system are sharp and strong with this mode of excitation, Fowler and Shaw[4] used active nitrogen as a source in obtaining the first accurate measurements of the heads of these bands. The system was also identified in the carbon arc in air, where it is responsible for most of the luminosity in the longer wave-length part of the visible spectrum. The appearance of the bands, however, is very different in this source. The heads are weak and masked by a great deal of overlapping rotational structure from adjacent bands. On the contrary, in the vacuum-tube and particularly in active nitrogen a large number of distinctly separated bands are seen, extending from the blue to the extreme red. The system has been traced as far as $\lambda 8134$ by Croze[5], and to $\lambda 9400$ by Asundi and Ryde.[5] Probably it extends far into the infrared. Each band shows four heads, degraded toward the red, that of shortest wave-length being very weak relative to the others.

As part of his pioneer work on the vibrational structure of band spectra, Heurlinger[6] assigned vibrational quantum numbers to the red system, and gave an equation for heads. The constants of the lower state agreed with those of the lower state of the violet CN bands, showing that these two band systems result from transitions to a common electronic configuration. Recently the vibrational numbering of the upper state of the red system has been changed as a result of the work of Asundi and Ryde.[5] The rotational structure of the violet system, for which accurate measurements[7] have been available since the early work of Kayser and Runge, was one of the first to which Heurlinger applied the quantum theory, and its interpretation is now well understood through the work of Kratzer, Dieke, Birge, and Mulliken.[8,9,10] The electronic transition is designated $^2\Sigma \rightarrow {}^2\Sigma$. The lower state of the red bands is therefore $^2\Sigma$, and is in all probability the normal state of CN. Evidence for this appears in the fact that the violet system can be self-reversed in the electric furnace.[11] The upper state of the red system is known to be $^2\Pi$, from various considerations including a study of the gross structure of the bands. The rotational analysis of the red system has not hitherto been

[2] R. J. Strutt, Proc. Roy. Soc. **85A,** 219 (1911); **88A,** 539 (1913).

[3] R. J. Strutt and A. Fowler, Proc. Roy. Soc. **86A,** 105 (1912).

[4] A. Fowler and H. Shaw, Proc. Roy. Soc. **86A,** 118 (1912).

[5] F. Croze, Comptes Rendus **150,** 1672 (1910). R. K. Asundi and J. W. Ryde, Nature **124,** 57 (1929).

[6] T. Heurlinger, Zeits. f. Physik **1,** 82 (1920).

[7] W. Jevons, Proc. Roy. Soc. **112A,** 407 (1926). Summary.

[8] A. Kratzer, Ann. d. Physik **71,** 72 (1923).

[9] R. T. Birge, Bull. Nat. Res. Council, No. 57, pp. 181–6.

[10] R. S. Mulliken, Phys. Rev. **30,** 138 (1927).

[11] A. S. King, Astrophys. J. **53,** 161 (1921).

attempted, perhaps because of the extreme complexity with which it is developed in the arc, from which high-dispersion spectra are most easily obtained. The analysis is nevertheless desirable, in order to study the properties and constants of the $^2\Pi$ state. A particular feature of this state requiring further investigation is the perturbation of the rotational levels $^2\Pi^{(6)}(J)$, which was discovered by Miss J. E. Rosenthal and one of the writers[12] in one of the first verifications of Kronig's theory of perturbations in band spectra. The present paper[13] contains the results of our analysis of the rotational structure, which was made possible by the use of grating plates of the red system as produced by active nitrogen.

Spectrograms

The source of light was the bright orange-colored flame obtained when carbon tetrachloride vapor is introduced slowly into a continuously flowing stream of active nitrogen. The rate of introduction was adjusted by a capillary leak to obtain the best intensity. Purification of the nitrogen previous to its activation was necessary, and consisted primarily in the removal of oxygen by passage through a tube of moist white phosphorous, and subsequent thorough drying. The form of the discharge tube and reaction chamber was smilar to that used in previous work with this type of excitation,[14] as were the conditions of pressure, rate of flow of nitrogen, etc. A detailed description of these will therefore be omitted here. As dispersing apparatus, the 21-foot Harvard grating was used in the first and second orders. Four sets of plates were obtained, covering the region 3500–8000A, each with two iron arc comparison spectra to eliminate the possibility of false shifts. Eastman Speedway plates were used for the region 3500–4900, Astronomical Green Sensitive plates for 4900–5800, Ilford panchromatic plates hypersensitized in ammonia for 5800–6850, and Speedway plates bathed in dicyanin for still longer wavelengths. Exposures were from 4 to 10 hours, constant temperature being maintained in the grating room.

Only the first order plates, with a dispersion varying from 1.91 to 1.95A per mm, were strong enough for satisfactory measurement.[15] The wavelengths were measured with reference to the international iron arc standards, from plates showing no relative shift of the two iron spectra. The complete rotational structure in seven of the strongest bands was measured, and also the band heads in 17 fainter ones. The agreements later obtained in the application of the combination principle indicate an accuracy of somewhat better than 0.01A for the measurements of the sharper lines.

[12] J. E. Rosenthal and F. A. Jenkins, Proc. Nat. Acad. Sci. **15,** 381 (1929).

[13] Preliminary report: F. A. Jenkins, Y. K. Roots and R. S. Mulliken, Phys. Rev. **38,** 1075 (1931). In this Letter we unfortunately used an incorrect v numbering in the $^2\Pi$ state, having overlooked the work of Asundi and Ryde.[5] We are indebted to Dr. W. Jevons for calling our attention to this. In the present account we have used the correct v numbering (cf. last paragraph of this paper.)

[14] For example, F. A. Jenkins and H. de Laszló, Proc. Roy. Soc. **122A,** 103 (1929).

[15] The (6,1), (6,2), and (7,3) bands were measured by the second writer (Y.K.R.) with a comparator at New York University, and the (4,1), (5,2), (6,2), and (8,3) bands with a Société Génévoise comparator at the University of California by the first writer (F.A.J.).

Rotational Structure

Term-formulas and permitted transitions

The spectral terms involved in $^2\Pi \rightarrow {}^2\Sigma$ bands, with an inverted $^2\Pi$ state intermediate between case (*a*) and case (*b*), are essentially as given by the following equations:[16]

$$\left.\begin{aligned}
{}^2\Pi_{3/2}: T_1'(J) &= T_e' + G' + B_v'\left\{(J+\tfrac{1}{2})^2 - 1 - \tfrac{1}{2}\left[4(J+\tfrac{1}{2})^2 - 4A/B_v' \right.\right. \\
&\quad \left.\left. + A^2/B_v'^2\right]^{1/2} + \overline{G^2}\right\} + \Phi_i(J) + D_v' J^4 + \cdots \\
{}^2\Pi_{1/2}: T_2'(J) &= T_e' + G' + B_v'\left\{(J+\tfrac{1}{2})^2 - 1 + \tfrac{1}{2}\left[4(J+\tfrac{1}{2})^2 - 4A/B_v' \right.\right. \\
&\quad \left.\left. + A^2/B_v'^2\right]^{1/2} + \overline{G^2}\right\} + \Phi_i(J) + D_v'(J+1)^4 + \cdots \\
{}^2\Sigma,\ J = K + \tfrac{1}{2}: T_1''(J) &= T_e'' + G'' + \tfrac{1}{2}\gamma K + B_v''(K+\tfrac{1}{2})^2 + D_v''(K+\tfrac{1}{2})^4 + \cdots \\
&= T_e'' + G'' + \tfrac{1}{2}\gamma(J-\tfrac{1}{2}) + B_v'' J^2 + D_v'' J^4 + \cdots \\
{}^2\Sigma,\ J = K - \tfrac{1}{2}: T_2''(J) &= T_e'' + G'' - \tfrac{1}{2}\gamma(K+1) + B_v''(K+\tfrac{1}{2})^2 + D_v''(K+\tfrac{1}{2})^4 + \cdots \\
&= T_e'' + G'' - \tfrac{1}{2}\gamma(J+\ ) + B_v''(J+1)^2 + D_v''(J+1)^4 + \cdots .
\end{aligned}\right\} \quad (1)$$

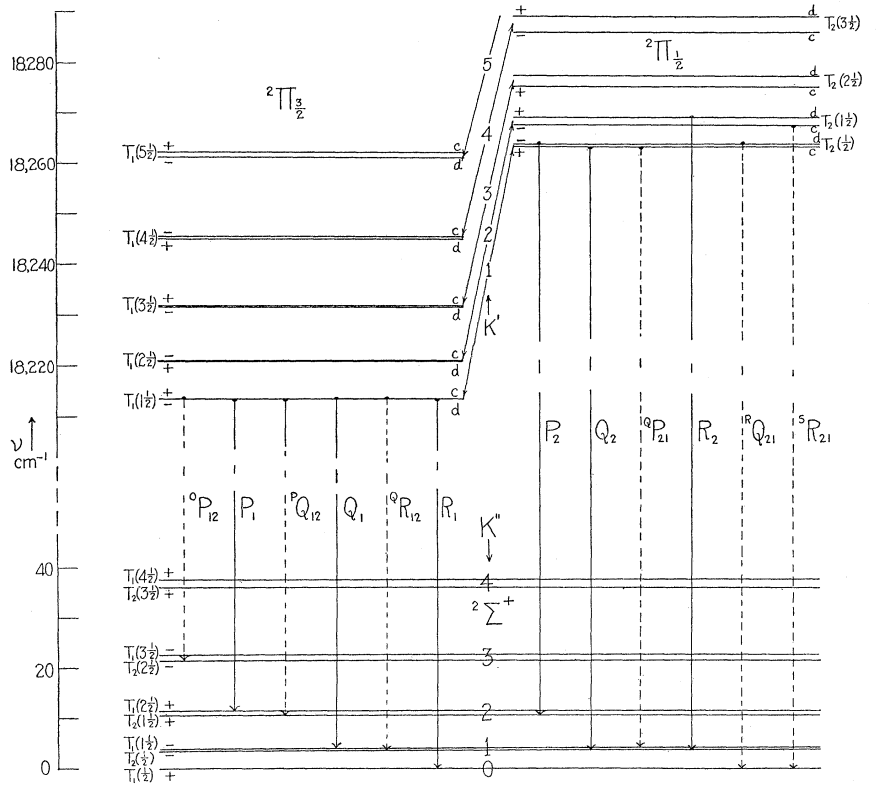

Fig. 1. Term-scheme for the 8,3 red CN band. The transition giving the first line in each branch is indicated by a vertical arrow. Satellite branches ($\Delta K \neq \Delta J$), and those with $\Delta K = 2$, are shown by dashed arrows. The spin doubling in $^2\Sigma$, and the Λ-doubling in $^2\Pi$, are magnified 50 times.

[16] **R. S. Mulliken,** Rev. Mod. Phys. **3,** 130 (1931); **2,** 109 (1930), with $\Lambda = 1$ for the $^2\Pi$ state.

For the $^2\Pi$ terms, A is the spin coupling constant, which in doublet states represents the electronic doublet separation for zero rotation. The small uncoupling term $\Phi_i(J)$ represents the splitting of each of the $^2\Pi$ rotational levels into two, designated T_c and T_d. Explicit equations of a somewhat complicated form can be given[17] for this term; they will be used below in the discussion of *Λ-doubling*. The additive constants $B_v(\overline{G}^2-1)$ cannot be found from the spectrum, since one can only evaluate the differences between terms. In the equation for the $^2\Sigma$ terms, the small constant γ measures the interaction of the electron spin with the magnetic field developed by the rotation of the molecule. It gives rise to a small separation of the two levels with $J=K\pm\frac{1}{2}$ associated with each value of K. Evidence for this in the present case will be considered later, under *spin doubling*.

The positive and negative symmetry properties of the terms $T(J)$ are important in determining the allowed transitions. The lower state in the present case is probably $^2\Sigma^+$, requiring a + designation for the lowest rotational level ($K=0$).[18] Applying the two selection rules $+\rightleftarrows-$ and $J\rightleftarrows J$, $J\pm1$, the + and − character of all the $^2\Pi$ rotational levels is easily found.[18] As shown in Fig. 1, there are twelve types of transitions allowed, giving rise to twelve branches in any one band. These are

$$
\begin{array}{cc}
^2\Pi_{3/2}\rightarrow{}^2\Sigma & ^2\Pi_{1/2}\rightarrow{}^2\Sigma \\
R_1(J)=T_{1d}'(J+1)-T_1''(J) & {}^SR_{21}(J)=T_{2c}'(J+1)-T_1''(J) \\
{}^QR_{12}(J)=T_{1c}'(J+1)-T_2''(J) & R_2(J)=T_{2d}'(J+1)-T_2''(J) \\
Q_1(J)=T_{1c}'(J)-T_1''(J) & {}^RQ_{21}(J)=T_{2d}'(J)-T_1''(J) \\
{}^PQ_{12}(J)=T_{1d}'(J)-T_2''(J) & Q_2(J)=T_{2c}'(J)-T_2''(J) \\
P_1(J)=T_{1d}'(J-1)-T_1''(J) & {}^QP_{21}(J)=T_{2c}'(J-1)-T_1''(J) \\
{}^OP_{12}(J)=T_{1c}'(J-1)-T_2''(J) & P_2(J)=T_{2d}'(J-1)-T_2''(J).
\end{array}
\qquad (2)
$$

In the bands under consideration, the 3/2-form branches ${}^SR_{21}$ and ${}^OP_{12}$, having $\Delta K=2$, are very weak, and could be measured only for the strongest bands. Also, since the separation of the terms $T_1''(K)$ and $T_2''(K)$ is very small, the $\frac{1}{2}$-form satellite branches could not be resolved from the corresponding main branches. As a result, the branches coalesce in pairs, as indicated by the brackets of Eqs. (2). Only eight branches are therefore measured for the strong bands, and six for the weaker ones.

Wave-numbers of band-lines

Table I contains the wave-numbers in vacuum of all the measured lines assigned to the band structure. For each branch which forms a head, the wave-length in I.A. of the head is given at the top of the appropriate column. In designating the branches in which coalescence occurs, the symbol of the satellite branch is omitted for brevity, although at low values of K it may

[17] R. S. Mulliken and A. Christy, Phys. Rev. **38**, 87 (1931).

[18] Reference 17, p. 103.

TABLE I

K''	*4, 1 band* λ 6332.159 R_2	Q_2	P_2	λ6347.036 R_1	λ6355.126 Q_1	P_1
0	15,785.52	—	—		—	—
1	786.77	15,781.69	—		15,731.00	—
2	787.64	779.04		15,742.35	731.22	
3	788.04	776.40	15,768.03	745.38	731.00	15,719.79
4	788.04	773.00	761.39	747.63	730.24	716.06
5	787.64	769.27	754.33	749.35	728.84	711.48
6	786.77	765.12	746.86	750.47	726.83	706.33
7	785.52	760.52	738.86	751.05	724.27	700.64
8	783.80	755.50	730.60	751.05	721.09	694.28
9	781.69	750.08	721.84	750.47	717.35	687.38
10	779.04	744.15	712.67	749.35	713.07	679.90
11	776.01	737.79	702.99	747.63	708.20	671.84
12	772.46	731.00	692.96	745.38	702.78	663.26
13	768.53	723.78	682.46	742.61	696.82	654.10
14	764.04	716.06	671.44	739.26	690.25	644.33
15	759.19	707.88	660.04	735.37	683.23	634.24
16	753.76	699.26	648.06	731.00	675.60	623.30
17	747.90	690.25	635.75	725.99	667.47	611.95
18	741.60	680.61	622.92	720.44	658.78	600.14
19	734.76	670.57	609.60	714.37	649.54	587.68
20	727.46	660.04	595.82	707.88	639.76	574.68
21	719.79	649.06	581.55	700.64	629.56	561.20
22	711.48	637.63	566.96	692.78	618.73	
23	702.78	625.63	551.74		607.40	
24	693.45	613.13			595.53	
25		600.14			583.18	
26		586.84			570.29	
27					566.88	

K''	*5, 2 band* λ6478.422 R_2	Q_2	P_2	λ6494.103 R_1	λ6502.318 Q_1	P_1
0	15,428.94	—	—		—	—
1	430.25	15,425.44	—	15,382.32	15,374.70	—
2	431.10	422.94		385.75	374.89	15,367.50
3	431.55	422.03	15,411.74	388.74	374.70	363.86
4	431.55	416.72	405.19	390.86	373.90	359.81
5	431.10	412.96	398.19	392.58	372.48	355.33
6	430.25	408.80	390.86	393.76	370.45	350.19
7	428.94	404.22	382.88	394.35	367.86	344.48
8	427.17	399.21	374.70	394.35	364.73	338.18
9	424.99	393.76	365.89	393.76	360.96	331.30
10	422.34	387.86	356.68	392.58	356.68	323.89
11	419.26	381.51	347.12	390.99	351.81	315.86
12	415.72	374.70	337.05	388.58	346.40	307.26
13	411.74	367.50	326.54	385.75	340.41	298.15
14	407.24	359.81	315.67	382.32	333.89	288.49
15	402.26	351.65	304.23	378.38	326.83	278.22
16	396.89	343.00	292.37	373.90	319.22	267.45
17	390.86	333.89	280.06	368.94	311.07	256.16
18	384.65	324.31	267.26	363.39	302.42	244.32
19	377.85	314.30	254.03	357.28	293.18	231.92
20	370.45	303.77	240.25	350.66	283.45	219.02
21	362.70	292.77	226.04	343.56	273.17	205.51
22	354.32	281.29	211.37	335.86	262.36	191.55
23	345.54	269.32	196.19	327.64	251.06	177.09
24	336.28	256.87	180.54	318.94	239.22	162.12
25	326.54	243.97		309.67	226.85	146.53
26		230.58		299.93	214.00	
27		216.62			200.63	
28		202.18			186.75	
29		187.27			172.51	

TABLE I. (*Continued*).

6, 1 band

K''	λ5232.629 $^{S}R_{21}$	λ5239.288 R_2	Q_2	P_2	λ5250.017 R_1	λ5254.869 Q_1	P_1	$^{O}P_{12}$
0			—	—	19,028.50	—	—	
1		19,080.52	19,075.67	—	032.33	19,024.69	—	
2		081.27	072.99	19,068.50	035.74	024.69	19,017.18	*Not*
3	19,095.99	081.27	069.89	061.75	038.44	024.69	013.61	*Observed*
4	098.77	081.27	066.60	055.23	040.40	023.36	009.53	
5	101.25	080.17	062.28	047.67	041.63	021.59	004.61	
6	103.24	078.88	057.66	039.92	042.27	019.17	18,999.13	
7	104.98	077.06	052.60	031.51	042.27	016.10	992.96	
8	105.55	074.70	047.02	022.48	041.63	012.39	986.05	
9	105.55	071.86	040.93	013.09	040.40	007.99	978.65	
10	105.55	068.50	034.34	003.15	038.44	003.15	970.55	
11	104.98	064.58	027.22	18,992.96	036.00	18,997.72	961.78	
12	103.75	060.19	019.63	982.46	032.33	*p* {991.98, 986.43}	952.49	
13	102.14	055.25	011.46	971.09	029.10	*p* {987.45, 982.46}	942.45	
14	099.56	049.79	002.86	959.34	024.69	976.18	931.82	
15	096.85	043.73	18,993.58	946.79	019.63	968.01	920.63	
16	093.67	037.22	983.78	934.02	014.14	960.06	908.82	
17		030.10	973.50	920.63	007.99	950.13	896.25	
18		022.48	962.69	906.49	001.17	940.24	883.33	
19		014.14	951.31	891.88	18,993.58	929.08	869.67	
20		005.48	939.38		986.05	918.56	855.48	
21		18,996.27	926.88		976.18	906.81	840.59	
22		986.43	913.88			894.45	825.37	
23			900.31			881.54		
24			886.19			868.01		
25			871.47					
26			856.24					
27			840.59					
28			824.08					

6, 2 band

K''	λ5849.347 $^{S}R_{21}$	λ5858.170 R_2	Q_2	P_2	λ5871.329 R_1	λ5877.643 Q_1	P_1	$^{O}P_{12}$
0	17,068.25	17,063.37	—	—	17,012.36	—	—	—
1	072.57	064.49	17,059.57	—	016.24	17,008.62	—	—
2	076.45	065.27	057.06	17,052.23	019.48	008.92	17,001.02	—
3	080.06	065.46	054.04	045.95	022.44	008.62	16,997.61	16,990.39
4	083.10	065.27	050.64	039.28	024.48	007.65	993.58	983.26
5	085.66	064.65	046.80	031.94	025.97	006.06	989.02	975.12
6	087.79	063.55	042.38	024.48	026.87	003.82	983.88	966.85
7	089.41	061.98	037.49	016.39	027.21	001.02	977.84	957.92
8	090.56	059.91	032.21	007.88	026.87	16,997.61	971.29	948.08
9	091.20	057.40	026.48	16,998.91	025.97	993.58	964.16	938.04
10	091.38	054.35	020.23	989.48	024.48	989.02	956.37	927.17
11	091.20	050.89	013.50	979.48	022.44	983.88	948.08	915.75
12	090.38	046.80	006.31	969.12	019.48	*p* {978.63, 973.78}	939.10	903.84
13	089.02	042.38	16,998.58	958.20	016.24	*p* {974.53, 969.60}	929.51	891.35
14	087.24	037.49	990.39	946.83	012.36	963.53	919.44 *p*	878.63
15	084.93	031.94	981.72	934.84	007.88	956.19	908.75 *p*	862.44
16	082.12	025.97	972.53	922.54	002.83	948.08	897.49	
17	078.79	019.48	962.83	909.80	16,997.26	939.41	885.60	
18	074.87	012.36	952.62	896.45	991.09	930.13	873.25	
19	070.53	004.93	941.91	882.51	984.41	920.26	860.27	
20	065.46	16,996.90	930.69	868.13	977.22	909.80	846.73	
21	060.94	988.39	918.98	853.21 *p*	969.60	898.86	832.67	
22		979.48	906.72	837.72 *p*	961.51	887.30	818.14	
23		969.86	893.95	*p*	954.66	875.19		
24	*p*	959.93	880.70			862.44		
25	*p*	949.81	866.85			849.21		
26			852.54			835.37		
27			837.72			820.93		

TABLE I. (*Continued*).

	7, 2 band							
	λ5347.480	λ5354.103			λ5365.018	λ5369.919		
K''	$^{S}R_{21}$	R_2	Q_2	P_2	R_1	Q_1	P_1	$^{C}P_{12}$
0	18,674.35	18,669.77	—	—	18,620.92	—	—	
1	678.89	671.08	18,666.10	—	624.60	18,616.72	—	
2	682.75	671.86	663.48	18,659.48	627.62	617.09	18,609.57	*Not*
3	686.11	672.09	660.35	652.63	630.23	616.72	605.98	*Observed*
4	688.89	671.86	656.73	646.14	632.14	615.56	601.78	
5	691.20	671.08	652.63	638.71	633.46	613.74	596.98	
6	693.07	669.77	648.01	631.19	634.10	611.31	591.48	
7	694.35	667.96	642.93	622.81	634.10	608.17	585.31	
8	595.21	665.64	637.31	614.08	633.46	604.47	578.48	
9	695.21	662.83	631.19	604.95	632.14	600.04	571.04	
10	695.21	659.48	624.60	595.09	630.23	595.09	562.97	
11	694.35	655.55	617.50	584.91	627.61	589.43	554.24	
12	693.07	651.15	609.89	574.23	624.35	583.16	544.87	
13	691.20	646.14	601.78	562.96	620.50	576.31	534.88	
14	688.89	640.70	593.13	551.10	616.02	568.69	524.27	
15		634.62	583.94	538.74	610.94	560.61	513.03	
16		628.04	574.23	525.88	605.21	551.86	501.20	
17		620.92	564.02	512.45	598.98	542.52	488.73	
18		613.25	553.24	498.50	592.09	532.56	475.66	
19		604.95	541.94	483.95	584.57	521.99	461.99	
20		596.21	530.06	468.90	576.31	510.81	447.74	
21		586.89	517.62	453.33	567.80	499.04	432.78	
22		576.97	504.67	437.14	558.48	486.69	417.36	
23		566.59	491.14	420.42	548.55	473.73	401.31	
24		555.52	477.06	403.16	538.06	460.17		
25		543.89	462.42		526.94	446.01		
26		531.72	447.52		515.26	431.34		
27		518.97	431.34		502.92	415.93		
28		505.66	415.09		490.11	400.04		
29		491.67			476.61			
30					462.41			

	7, 3 band					
	λ5992.645			λ6006.053	λ6012.472	
K''	R_2	Q_2	P_2	R_1	Q_1	P_1
0	16,680.21	—	—		—	—
1	681.45	16,676.51	—	16,634.86	16,627.19	—
2	682.37	673.90		638.18	627.50	16,620.29
3	682.51	670.86		640.83	627.19	616.48
4	682.37	667.36	16,656.60	643.06	626.18	611.90
5	681.87	663.41	649.14	644.35	624.57	607.76
6	680.77	659.05	642.33	645.03	622.31	602.46
7	679.19	654.17	633.97	645.27	619.46	596.55
8	677.16	648.88	625.46	645.03	615.99	589.97
9	674.61	643.06	616.70	643.93	611.90	582.84
10	671.63	636.85	607.19	642.33	607.19	575.10
11	668.13	630.07	597.52	640.14	601.98	566.83
12	664.13	622.92	587.23	637.32	596.13	557.91
13	659.65	615.25	576.31	633.97	589.67	548.28
14	654.64	607.19	565.01	630.07	582.69	538.18
15	649.14	598.42	553.17	625.46	575.10	527.49
16	643.06	589.29	540.88	620.29	566.83	516.19
17	636.60	579.60	528.03	614.63	558.11	504.35
18	629.59	569.47	514.67	608.30	548.75	491.90
19	621.97	558.82	500.90		538.88	
20	613.87	547.66	486.50		528.41	
21	605.30	535.97			517.37	
22		523.77			505.78	
23		511.04			493.63	
24		497.83			480.90	

TABLE I. (*Continued*).

	8, 3 band							
	λ5466.306	λ5473.289			λ5484.921	λ5489.950		
K''	$^{S}R_{21}$	R_2	Q_2	P_2	R_1	Q_1	P_1	$^{O}P_{12}$
0	18,268.45	18,263.65	—	—	18,213.58	—	—	—
1	272.63	264.76	18,259.95	—	217.45	18,209.61	—	—
2	276.44	265.49	257.36		220.59	210.06	18,202.61	—
3	279.74	265.49	254.30	18,246.52	223.17	209.61	199.07	
4	282.55	265.15	250.74	239.65	225.03	208.43	194.91	18,184.26
5	284.86	264.28	246.70	232.44	226.24	206.65	190.08	176.67
6	286.58	262.91	242.13	224.65	226.75	204.25	184.61	167.83
7	287.82	261.03	237.07	216.57	226.75	201.09	178.51	158.87
8	288.57	258.64	231.51	207.82	225.99	197.29	171.69	149.11
9	288.82	255.72	225.44	198.60	224.65	192.96	164.23	138.64
10	288.57	252.28	218.85	188.80	222.64	187.92	156.17	127.57
11	287.82	248.34	211.73	178.51	220.01	182.26	147.49	115.83
12	286.37	243.85	204.07	167.83	216.75	175.98	138.12	103.55
13	284.45	238.84	195.97	156.55	212.86	169.08	128.16	090.52
14	281.94	233.28	187.27	144.68	208.43	161.55	117.57	076.86
15	279.03	227.18	178.03	132.37	203.27	153.40	106.39	062.59
16	275.51	220.59	168.28	119.48	197.50	144.68	094.60	047.84
17	271.36	213.36	157.98	106.10	191.20	135.29	082.14	032.40
18	266.77	205.61	147.15	092.08	184.26	125.31	069.08	016.28
19		197.29	135.77	077.62	176.67	114.76	055.42	17,999.73
20		188.44	123.83	062.59	168.53	103.55	041.23	982.66
21		179.03	111.32	047.02	159.77	091.78	026.37	964.64
22		169.08	098.28	030.87	150.43	079.41	010.95	946.31
23		158.53	084.68	014.19	140.46	066.45	17,994.96	927.11
24		147.49	070.55	17,996.94	129.90	052.89	978.29	907.48
25		135.77	055.84	979.13	118.77	038.76	961.07	
26		123.58	040.59	960.85	107.01	024.02	943.27	
27		110.77	024.77	941.89	094.60	008.64	924.85	
28		097.39	008.36	922.42	081.74	17,992.74	905.88	
29		083.47	17,991.42	902.40	068.23	976.25	886.26	
30		069.08	973.93	881.75	18,054.12	959.15	866.09	
31		053.93	955.83	860.66	039.40	941.43		
32		038.30	937.20		024.02	923.16		
33		022.07	917.96		008.36	904.29		
34		005.26	898.17			884.85		
35		17,987.83	877.89			864.82		
36		969.69						

contribute a considerable part of the intensity. The first wave-number in the column headed R_2 should be denoted $^{R}Q_{21}(0)$, since the line $R_2(0)$ is missing (cf. Fig. 1). Each branch in the stronger bands has been found to begin with the value of K'' expected from Fig. 1, with the possible exception of the P_2 branch, the first lines of which are extremely weak. Thus in the 8,3 band, the line $P_2(2)$ was not found, although its expected position is free from other lines. On the whole, however, the evidence from the missing lines is definite, and shows that the $^2\Pi$ state must be inverted, since there is a greater number of missing lines in the low-frequency sub-band.

The appearance of the bands under high dispersion is shown in Fig. 2, in which one typical regular band, 8,3, and one which shows marked perturba-

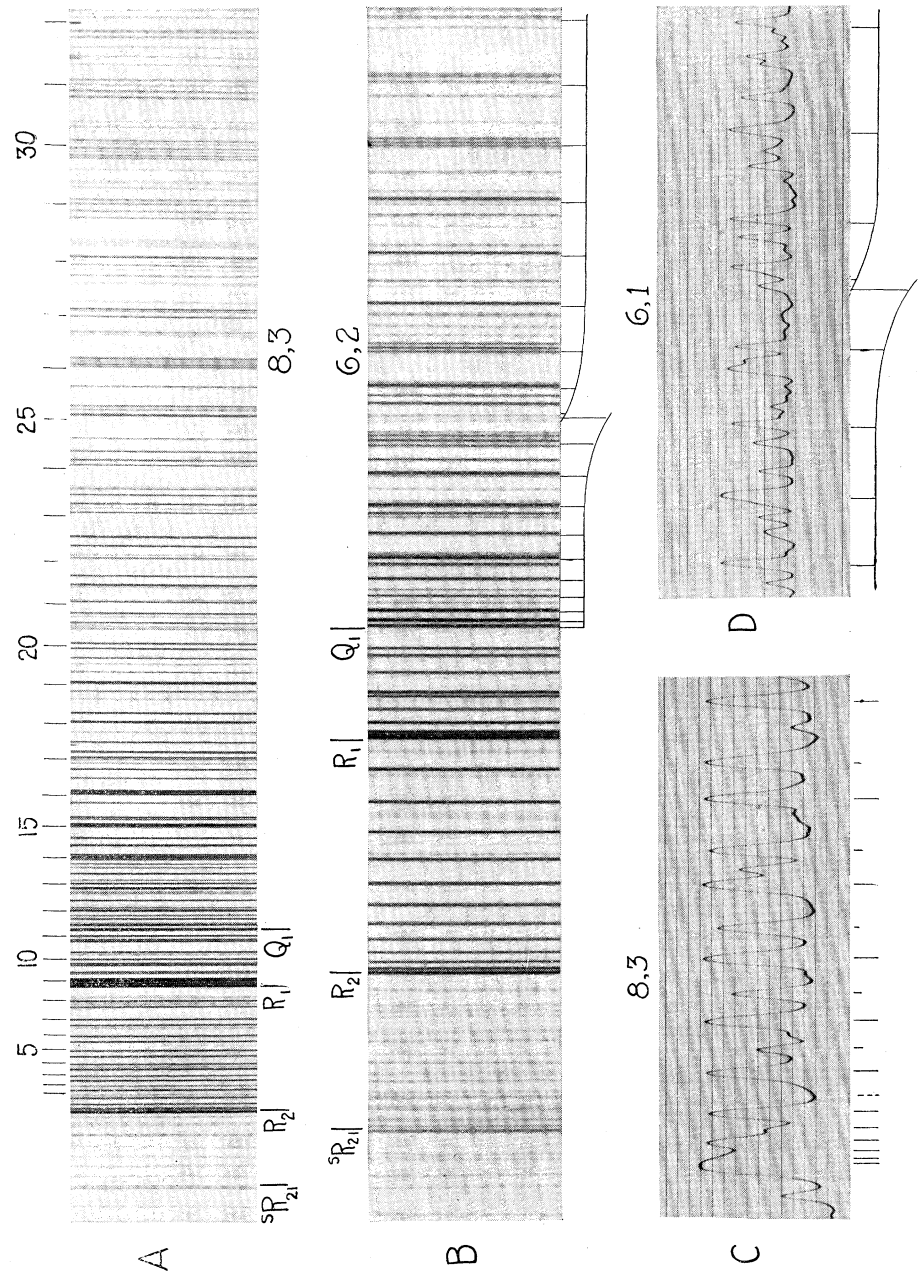

Fig. 2. Bands of the red CN system. *A*. The 8,3 band. The four heads are marked below. Above, the Q_2 lines are designated, and numbered with the values of K''. Wave-lengths increase to the right. *B*. The 6,2 band, enlarged somewhat more than the 8,3 band in *A*. The perturbed branch Q_1 is marked below. Displacements of the lines toward the red or toward the violet are indicated by a rise or fall of the otherwise horizontal connecting line. *C*. Microphotometer curve of the first part of the 8,3 band. The position of the single missing line between the two strong branches R_2 (long lines) and Q_2 (short lines) is indicated by the dotted line. *D*. Microphotometer curve of the main perturbation in the 6,1 band, corresponding to that shown in *B* for the 6,2 band.

tions, 6,2, are reproduced. The irregularities and "extra" lines which occur in the regions of perturbations are designated in Table I by p and will be considered in detail below. In Fig. 2c, a microphotometer trace is given of the first part of the 8,3 band, to show the single missing line occurring between ${}^{R}Q_{21}(0)$ and $Q_2(1)$. A Fortrat diagram of this band is given in Fig. 3. The 8,3 band was chosen as a representative strong band in which there is a minimum of overlapping, and which contains no perturbations.

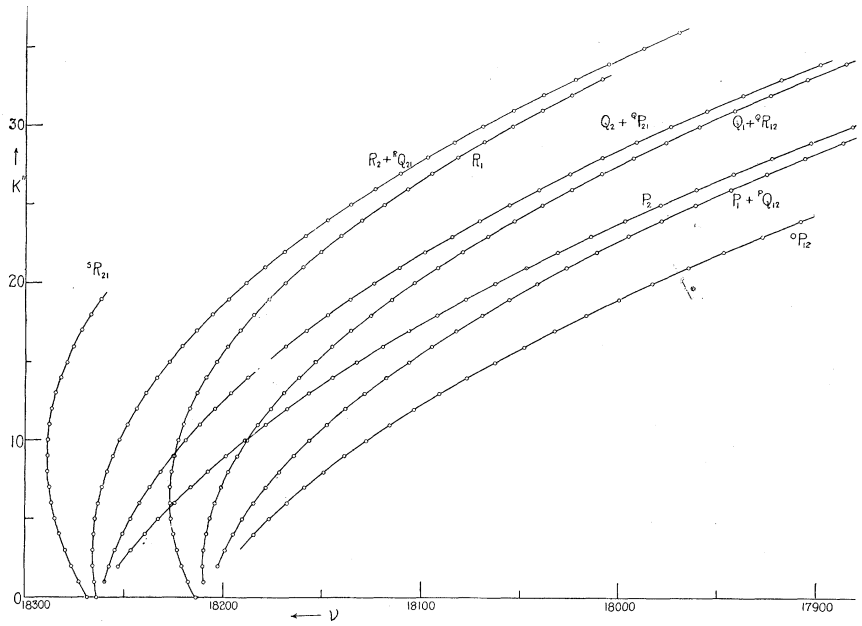

Fig. 3. Fortrat diagram of the 8,3 band. The circles are experimental values, while the curves have been drawn according to the theoretical Eq. (1), using the constants given in Table IV. The largest deviation from experiment is one-tenth the diameter of one of the small circles, hence less than the accuracy of drawing the curves.

Line intensities

Instead of giving visual intensity estimates of all the lines, as is usual, we have preferred to study the intensity relations in the typical 8,3 band in a more quantitative way. The original plates were not calibrated with density marks, and since they were color-sensitized the form of the characteristic curves is very uncertain. Considerable information can, however, be obtained from a study of the photographic densities of the lines, since this at least gives the proper order of intensities. Fig. 4 gives the density, or logarithm of the opacity, of every unblended line in the 8,3 band, measured on a green sensitive plate which was developed about 4 minutes in metol-hydroquinone. The opacities of the line centers were obtained with a Zeiss-Koch recording microphotometer, having the slit much narrower than the width of a line.

The intensities of the several branches should be given by the theoretical

formulas derived by Hill and Van Vleck.[19] Qualitatively, the observed relations are those to be expected if the superposition of the satellite branches on the corresponding main branches is taken into account. The $^2\Pi$ state is intermediate between Hund's case (*a*) and case (*b*), with the result that for very low J the case (*a*) intensity relations are approximated, while for large rotation, we have very nearly case (*b*). In strict case (*a*) the twelve branches of Eqs. (2) are of comparable intensities, the order being $Q_i > R_i > P_i$. In case (*b*), however, the $^SR_{21}$ and $^OP_{12}$ branches, with $\Delta K = 2$, are strictly forbidden, and the satellites $^QR_{12}$, $^PQ_{12}$, $^RQ_{21}$ and $^QP_{21}$ with $\Delta K \neq \Delta J$, are very weak. In Fig. 4 it will be seen that the $^SR_{21}$ and $^OP_{12}$ branches are weakest of all, and

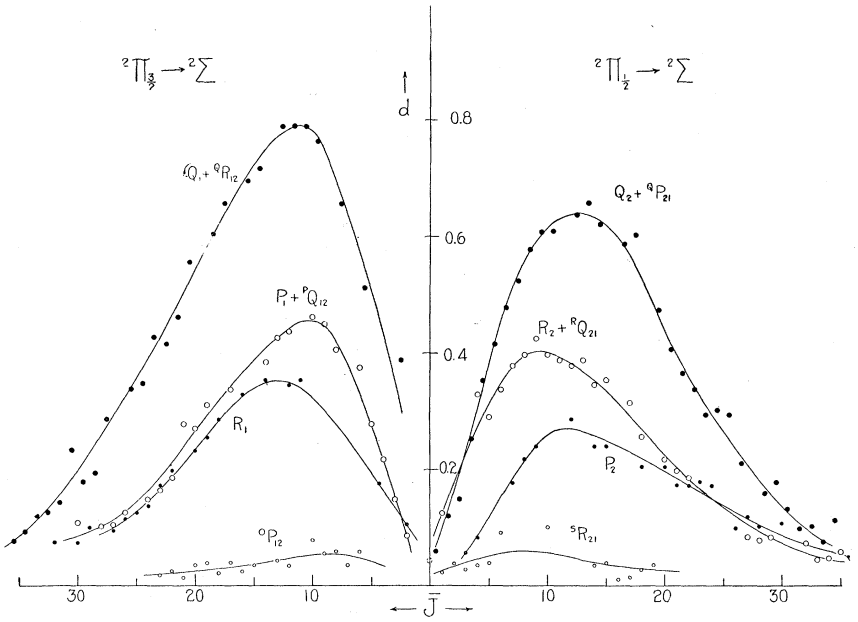

Fig. 4. Photographic densities in the 8,3 band. The densities d of all lines which are not known to be blended are plotted against $\bar{J}$, the mean J in the upper and lower states.

fade out very soon with increasing J. However, at the lowest values of J, the $^SR_{21}$ branch is fairly strong, and in several bands its first line, $^SR_{21}(0)$ could easily be measured. This results from the fact that for very small rotation case (*a*) is approached. In the branches in which coalescence with a satellite occurs, we find at first a very rapid rise of intensity, where the satellite branch is strong, then a more gradual falling off after the satellite has decreased to the very low intensity characteristic of case (*b*). The R_1 and P_2 branches, on the other hand, are weaker at first, but at the highest J have become practically equal to R_2 and P_1, respectively, as the intensity formulas for case (*b*) require. Fig. 4 shows that the total intensity of $^2\Pi_{3/2} \rightarrow {}^2\Sigma$ is distinctly greater

[19] E. L. Hill and J. H. Van Vleck, Phys. Rev. **32,** 267 (1928). Cf. also the review by R. S. Mulliken, Rev. Mod. Phys. **3,** 94 (1931), sections *J2c, J2d, J3,* and Fig. 29.

than that of $^2\Pi_{1/2} \rightarrow {}^2\Sigma$. This appears to be in agreement with the intensity equations of Hill and VanVleck if the $^2\Pi_{1/2}$ and $^2\Pi_{1\ 1/2}$ levels are initially about equally populated.[19]

Rotational terms of the $^2\Sigma$ state

Because of the double character of all the rotational terms in $^2\Pi$ and $^2\Sigma$ states, the combination principle as applied within any one band does not yield more than a single value for a given term-difference. Exact agreements are expected only when an identical term-difference is evaluated from two bands with a common vibrational state. This requirement will be found to be fulfilled for all of the bands in Table I. As an example, we quote in Table II the values of the differences

$$R_1(K-1) - P_1(K+1) = \Delta_2 F_1''(K),$$

TABLE II. *Combination differences $\Delta_2 F_1''$ for the $^2\Sigma$ state.*

K	$^2\Pi \rightarrow {}^2\Sigma$ 4, 1	6, 1	$^2\Sigma \rightarrow {}^2\Sigma$ 1, 1, (U &P)	0, 1(H)	$^2\Pi \rightarrow {}^2\Sigma$ 5, 2	6, 2	$^2\Sigma \rightarrow {}^2\Sigma$ 1, 2 (H)
3	—	18.72	18.85	18.74	18.46	18.63	18.82
4	26.29	26.21	26.04	26.21	25.94	26.25	26.09
5	33.90	33.83	33.63	33.74	33.41	33.42	33.42
6	41.30	41.27	41.21	41.21	40.67	40.60	40.84
7	48.71	48.67	48.76	48.69	48.10	48.13	48.26
8	56.19	56.22	56.22	56.21	55.58	55.58	55.64
9	63.67	63.62	63.58	63.60	63.05	63.05	62.98
10	71.15	71.08	71.17	71.15	70.46	70.50	70.42
11	78.63	78.62	78.53	78.62	77.90	77.89	77.80
12	86.09	85.95	86.23	86.18	85.32	85.38	85.16
13	93.53	93.55	93.69	93.61	92.84	92.93	92.57
14	101.05	100.51	101.01	101.06	100.09	100.04	99.92
15	108.37	108.47	108.55	—	107.53	107.49	107.41
16	115.96	115.87	115.85	116.08	114.87	114.87	114.81
17	123.42	123.38	123.38	—	122.22	122.28	122.06
18	130.86	130.81	130.81	—	129.58	129.58	129.71

as found from the bands with $v''=1$ and 2. The violet CN bands, having the same lower state, also give values of $\Delta_2 F''$ for $v=1$ and 2, and these are given in the table for comparison.[20] Data for the violet bands are from Heurlinger,[21] and from Uhler and Patterson.[22]

Since the rotational terms of the lower state are identical with those already known from the violet bands, no new information about them can be derived from the red bands, except in regard to the spin doubling, as discussed below. Our data include bands with $v''=1$, 2 and 3, and the rotational constants have been computed, with the hope of improving the accuracy for states 2 and 3, for which the data from the violet bands are poor. Treating the

[20] Since the spin doublets in the violet bands are not resolved for low K, the combination differences represent the mean of $\Delta_2 F_1$ and $\Delta_2 F_2$. This should differ from $\Delta_2 F_1$ itself only slightly.

[21] T. Heurlinger, Dissertation, Lund (1918).

[22] H. S. Uhler and R. A. Patterson, Astrophys. J. **42**, 434 (1915).

combination differences in the usual manner by the method of least squares, we find the following values of B_v'': $B_1''=1.8731$, $B_2''=1.8558$, $B_3''=1.8384$, from which we obtain

$$B_v'' = 1.8991 - 0.01735(v'' + \tfrac{1}{2}).$$

This agrees well with the equation obtained from the violet bands by Heurlinger[21]:

$$B_v'' = 1.9002 - 0.0173(v'' + \tfrac{1}{2}).$$

The slight difference in B_e'' is probably due to different methods of evaluation. In our computation, the term in D_v'' was corrected for by using the values from the equation

$$D_v'' = -6.401 \times 10^{-6} - 0.00949(v'' + \tfrac{1}{2}) \times 10^{-6},$$

which results from the theoretical relations between D_e, β, ω_e, α_e, and x_e.[23] Further information about the constants of the $^2\Sigma$ state could be obtained by measuring other bands with higher v'', but we have not undertaken to do this.

Spin doubling in the $^2\Sigma$ state

The violet bands permit us to determine only the difference between the spin doublings, i.e., the separations of $F_1(K)$ and $F_2(K)$, in the upper and lower $^2\Sigma$ states. From $^2\Sigma \rightarrow {}^2\Sigma$ bands, the absolute value of the spin doubling cannot be found in either state, because only $F_1 \rightarrow F_1$ and $F_2 \rightarrow F_2$ transitions occur. The red bands should yield the actual doubling in the lower state. It is extremely small, however, and the satellite branches are in no case resolved from the main branches. Evidence for the doubling is found, however, in the fact that at high values of K a slight difference is found in the combination differences, such that

$${}^{S}R_{21}(K-1) - \begin{Bmatrix} Q_2 \\ {}^{Q}P_{21} \end{Bmatrix}(K+1) < \begin{Bmatrix} R_2 \\ {}^{R}Q_{21} \end{Bmatrix}(K-1) - P_2(K+1)$$

and

$$\begin{Bmatrix} Q_1 \\ {}^{Q}R_{12} \end{Bmatrix}(K-1) - {}^{O}P_{12}(K+1) < R_1(K-1) - \begin{Bmatrix} P_1 \\ {}^{P}Q_{12} \end{Bmatrix}(K+1).$$

Since all of the lines in each inequality come from the same upper state, this can only result from a doubling in the lower state. We can assume that the satellites are of negligible intensity at high K, where the inequality is appreciable. The doubling is then found from the relations

$$\begin{aligned} &[R_1(K-2) - P_1(K)] - [Q_1(K-2) - {}^{O}P_{12}(K)] \\ &= [R_2(K) - P_2(K+2)] - [{}^{S}R_{21}(K) - Q_2(K+2)] \\ &= F_1''(K) - F_2''(K) = \gamma_0(K + \tfrac{1}{2}). \end{aligned}$$

On plotting these differences, they appear to be linear in K within experimental error, and the resulting values of γ_0 are, for $v''=3$, $\gamma_0=+0.0071$, for

[23] E. C. Kemble, Jour. Opt. Soc. Am. **12**, 1 (1926). Cf. also F. A. Jenkins, Phys. Rev. **35**, 327 (1930).

$v''=2$, $\gamma_0=+0.0082$. Hence $F_1>F_2$, as usually occurs, and the splitting is of the same order of magnitude as the actual doubling of the lines in the violet bands, which in the 0,0 band amounts to 0.0090 $(K''+\frac{1}{2})$ for low K.[24] Unfortunately do data are available for the doubling in the violet bands with $v''=2$ and 3, so that the term-splitting in the upper $^2\Sigma$ state cannot be evaluated.

Rotational terms of the $^2\Pi$ state

The combination relations yield term differences Δ_2F_i' which refer either to the T_c or to the T_d terms, as will be evident from the energy levels of Fig. 1. The differences Δ_2F_{ic}', obtained by using the $^SR_{21}$ and $^OP_{12}$ branches, are slightly less than the true values, because of the spin doubling in the lower state. Hence only the values of Δ_2F_{id}', obtained from the main branches, have been used in calculating the constants. These are also more accurate because of the greater intensity of the lines involved. In every case the application of the combination principle gives term-differences showing the proper relations if it is assumed that in the $^2\Pi$ states $T_{2d}>T_{2c}$ and $T_{1c}>T_{1d}$ for low J, and in the $^2\Sigma$ state $T_1>T_2$ throughout. An example of the agreement of combination differences in the upper state is given in Table III, derived from the 6,1 and 6,2 bands.

TABLE III. *Exact and approximate combination differences Δ_2F_i' for the $^2\Pi$ state, $v'=6$.*

J	*6, 1 band* $R_2(J)-P_2(J)$	$R_1(J)-P_1(J)$	$^SR_{21}(J)-Q_2(J-1)$	*6, 2 band* $R_2(J)-P_2(J)$	$R_1(J)-P_1(J)$	$^SR_{21}(J)-Q_2(J-1)$	$Q_1(J+1)$ $^OP_{12}(J)$
$1\frac{1}{2}$	12.77			13.04		13.00	
$2\frac{1}{2}$	19.52	18.56		19.51	18.46	19.39	18.23
$3\frac{1}{2}$	26.04	24.83	26.10	25.99	24.83	26.02	24.39
$4\frac{1}{2}$	32.50	30.87	32.17	32.71	31.25	32.46	30.84
$5\frac{1}{2}$	38.96	37.02	38.97	39.07	36.95	38.86	36.97
$6\frac{1}{2}$	45.55	43.14	45.58	45.59	42.99	45.41	43.10
$7\frac{1}{2}$	52.22	49.31	52.38	52.03	49.37	51.92	49.53
$8\frac{1}{2}$	58.25	55.58	58.53	58.49	55.58	58.35	55.54
$9\frac{1}{2}$	65.35	61.75	64.62	64.87	61.81	64.72	61.85
$10\frac{1}{2}$	71.62	67.89	71.21	71.41	68.11	71.15	68.13
$11\frac{1}{2}$	77.73	74.22	77.76	77.68	74.36	77.70	74.79p
$12\frac{1}{2}$	84.16	79.84	84.12	84.18	80.38	84.07	78.25p
$13\frac{1}{2}$	90.45	86.65	90.68	90.66	86.73	90.44	84.90p
$14\frac{1}{2}$	96.94	92.87	96.70	97.10	92.92	96.85	93.75p
$15\frac{1}{2}$	103.20	99.00	103.27	103.43	99.13	103.21	
$16\frac{1}{2}$	109.47	105.32	109.89	109.68	105.34	109.59	
$17\frac{1}{2}$	115.99	111.74		115.91	111.66	115.96	
$18\frac{1}{2}$	122.26	117.84		122.42	117.84	122.25	
$19\frac{1}{2}$		123.91		128.77	124.14	128.62	
$20\frac{1}{2}$		130.57		135.18	130.49		

In determining the constants we have used the fact that for low values of J, the following term-formulas are approximately valid:[25]

[24] R. T. Birge, Astrophys. J. **55**, 280 (1922).

[25] R. S. Mulliken, Rev. Mod. Phys. **3**, 116 (1931), and Eqs. (47), (46) in **2**, 113–4 (1930).

$$
\begin{aligned}
{}^2\Pi_{3/2}: T_1(J) &= C + B^*_{v,+1/2}[(J+\tfrac{1}{2})^2 - (\tfrac{3}{2})^2] + D^*_{v,+1/2}(J+\tfrac{1}{2})^4 + \cdots \\
{}^2\Pi_{1/2}: T_2(J) &= C + B^*_{v,-1/2}[(J+\tfrac{1}{2})^2 - (\tfrac{1}{2})^2] + D^*_{v,-1/2}(J+\tfrac{1}{2})^4 + \cdots ,
\end{aligned} \tag{3}
$$

where C is a constant depending on the value of v. In these expressions $B_{v,\Sigma}{}^*$ is the "apparent" value of B_v which is obtained by assuming that the low rotational terms have the form characteristic of case (a). It is connected[25] with the true value of B_v by the relation

$$B^*_{v,\pm 1/2} = B_v(1 \pm B_v/A\Lambda). \tag{4}$$

To evaluate $B^*_{v\,\Sigma}$, for the various values of v, we investigate the quantities

$$
\begin{aligned}
\Delta_2 F_i'(J) &= F_i'(J+1) - F_i'(J-1) \\
&= 4B^*_{v,\Sigma}(J+\tfrac{1}{2}) + 8D^*_{v,\Sigma}(J+\tfrac{1}{2})^3 + \cdots .
\end{aligned}
$$

Since the second term is small, we can assume without appreciable error that $D^*_{v,\Sigma} = D_v = D_e + \beta(v+\frac{1}{2})$, where D_e is given by the well-known relation[23]

$$D_e = -4B_e{}^3/\omega_e{}^2.$$

Using preliminary values of B_e, ω_e, and of the quantities required for calculating β, one can compute the term $8D_v(J+\frac{1}{2})^3$, subtract from the quantities $\Delta_2 F_1'(J)$, and, dividing by $J+\frac{1}{2}$, obtain

$$[\Delta_2 F_i'(J) - 8D_v(J+\tfrac{1}{2})^3]/(J+\tfrac{1}{2}) = 4B^*_{v,\Sigma}.$$

This quantity is nearly independent of J, and extrapolation to $J=0$ gives the $B^*_{v,\Sigma}$ values represented by Eq. (4). The mean of $B^*_{v,+1/2}$ and $B^*_{v,-1/2}{}^*$ then gives the true value of B_v. The evaluation was carried out graphically, as illustrated in Fig. 5. Strictly, the extrapolation should have been carried out to

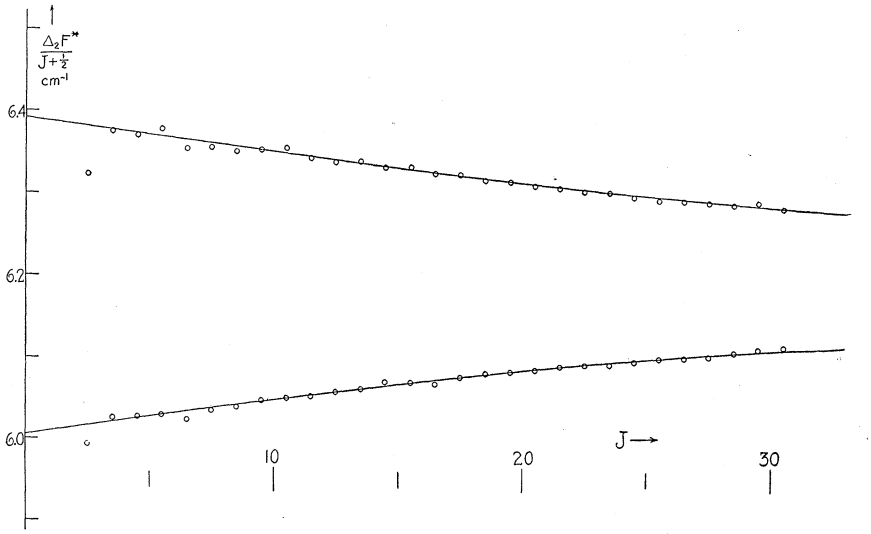

Fig. 5. Illustrating the graphical determination of $B^*_{v,\Sigma}$.

zero rotation, rather than to $J=0$. The difference, especially in B_v, is, however, slight, and unfortunately not exactly determinable. The resulting constants are given in Table IV, in which are also included the constants of the lower state, and the molecular constants derived from these.

TABLE IV. *Constants of the band structure.* All quantities are in cm^{-1} units, except I_e and r_e. Strictly speaking, the B^* values apply only to the d rotational levels.

v'	$B^*_{v,+\frac{1}{2}}$	$B^*_{v,-\frac{1}{2}}$	$B^*_{v,+\frac{1}{2}}-B^*_{v,-\frac{1}{2}}$	B_v'	$-D_v'\times10^6$	p_0	$-q_0$	$-A$	$2B_v^2/A$
4	1.5705	1.6727	−.1022	1.6215	6.140	0.00621	0.000252	52.14	−.1009
5	1.5490	1.6522	−.1032	1.6005	6.153	0.00853	0.000365	52.33	−.0979
6	1.5360	1.6352	−.0992	1.5855	6.166	—	—	52.52	−.0957
7	1.5140	1.6237	−.1097	1.5687	6.178	—	—	50.89	−.0967
8	1.5017	1.5990	−.0973	1.5502	6.191	0.01872	0.000435	51.65	−.0931

v''	B_v''	$-D_v''\times10^6$	γ_0		B_e	α	D_e	β	I_e	r_e
1	1.8731	6.415	—	$^2\Pi$	1.6990	0.01746	−6.133	−1.27	16.28	1.236
					±0.001	±0.002	$\times10^{-6}$	$\times10^{-8}$	$\times10^{-40}$ g cm	$\times10^{-8}$ cm
2	1.8558	6.425	0.0082	$(A=-52.2)$						
					1.8991	0.01735	−6.401	−0.949	14.56	1.169
3	1.8384	6.435	0.0071	$^2\Sigma$	±0.0005	±0.001	$\times10^{-6}$	$\times10^{-8}$	$\times10^{-40}$ g cm	$\times10^{8}$ − cm

The column headed $-A$ gives the experimental values of the electronic separation in the $^2\Pi$ state. They were determined from the relation[26]

$$|A| = T_2'(\tfrac{1}{2}) - T_1'(1\tfrac{1}{2}) + B_v' - 3B_v'^2/|A| .$$

The variation in A for the different vibrational states is regarded as real, since independent results for this constant from different bands with the same upper state agreed closely. Thus the 6,2 and 6,1 bands gave 52.50 and 52.55, respectively, while the 7,3 and 7,2 bands gave 50.97 and 50.81. The high value for $v'=6$, and the low value for $v'=7$ are undoubtdely connected with the perturbation effects described below.

We have adopted $A=-52.20$ as the most probable value of the coupling constant. In Table IV the differences $B^*_{v,+1/2}-B^*_{v,-1/2}$* are compared with their theoretical values from Eq. (4), namely $2B_v^2/A$. The agreement is satisfactory, both in their magnitude and in their decrease with v', but the perturbations in A invalidate any more quantitative conclusions. The slight discrepancies between observed and calculated values can be attributed, at least partly, to the uncertainty already noted in connection with the extrapolations to get the B_v* values. The constants B_v are represented within experimental error by the equation

$$B_v = B_e - \alpha(v+\tfrac{1}{2}).$$

The results for B_e and α are included in Table IV, as well as the moment of inertia, I_e, and the internuclear distance r_e in the equilibrium position. As a rigorous test of the term-equations (1), we have computed the terms and observed frequencies for the 8,3 band, using the constants given in Table IV. As expected, slight systematic discrepancies are found at high values of K, which can be further reduced by slight adjustments of the constants. They are of the order of 0.2 cm^{-1} at $K=30$, and entirely negligible on the scale to which the Fortrat diagram of Fig. 3 is drawn.

[26] R. S. Mulliken, Phys. Rev. **33**, 747 (1929).

Λ-doubling in the $^2\Pi$ state

The term $\Phi_i(J)$ in the energy formulas (1) is double-valued for each component of the $^2\Pi$ state. This gives rise to four series of terms T_{1c}, T_{1d}, T_{2c} and T_{2d}, the subscripts c and d having the theoretical significance assigned to them by Mulliken.[27] The separation of T_{1c} from T_{1d}, and of T_{2c} from T_{2d} is small and represents the Λ-doubling. It is defined as the difference

$$\Delta\nu_{dc} = T_d(J) - T_c(J).$$

In the present case we can evaluate it from the relations

$$[R_2(J) - Q_2(J)] - [Q_2(J+1) - P_2(J+1)] \sim 2\Delta\nu_{2dc}(J+\tfrac{1}{2}) \text{ for } {}^2\Pi_{1/2};$$
$$[R_1(J) - Q_1(J)] - [Q_1(J+1) - P_1(J+1] \sim 2\Delta\nu_{1dc}(J+\tfrac{1}{2}) \text{ for } {}^2\Pi_{3/2}.$$

Fig. 6 shows graphically the observed $\Delta\nu_{dc}$ in the initial states $v'=4$ to 8. For $v'=4$, 5, and 8 it takes the form known to be characteristic of $^2\Pi$ states intermediate between case (*a*) and case (*b*). As has been shown by Mulliken and

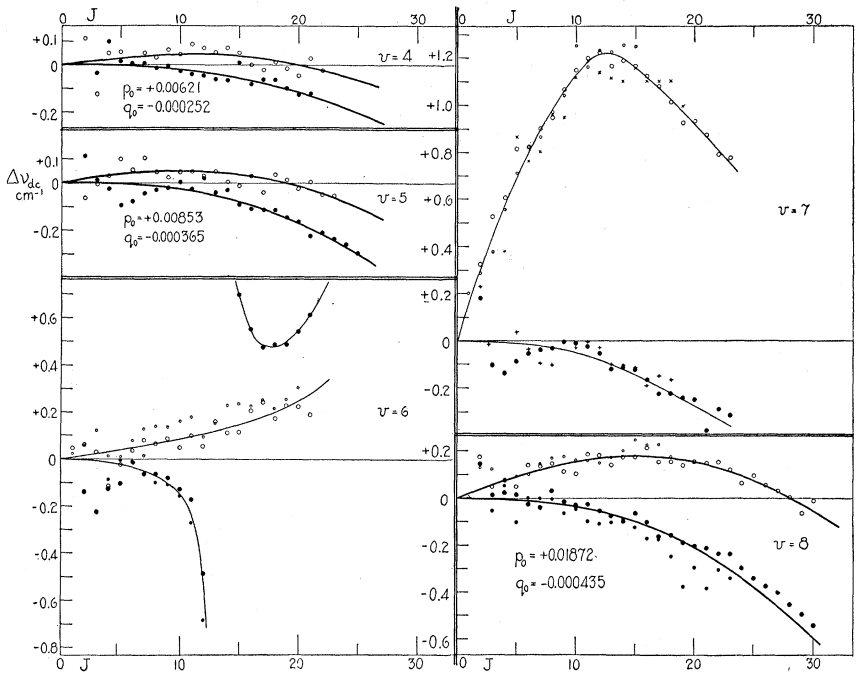

Fig. 6. Λ-doubling in the $^2\Pi$ state. The heavy curves in the cases $v'=4$, 5 and 8 are the theoretical curves, with the coefficients given. For the perturbed states $v'=6$ and 7, the curves are empirically drawn. Large dots and large circles are values of $\Delta\nu_{1dc}$ ($^2\Pi_{3/2}$) and $\Delta\nu_{2dc}$ ($^2\Pi_{1/2}$) obtained from the main branches. Small dots and circles are values whose determination involved the fainter branches $^SR_{21}$ and $^OP_{12}$. In the $v'=7$ figure, crosses are data from the 7,3 band, dots and circles from the 7,2 band. All data for $v'=6$ are from the 6,2 band.

[27] R. S. Mulliken, Rev. Mod. Phys. **3**, 94 (1931).

Christy,[17] the theoretical work of Van Vleck on Λ-doubling leads to the following expressions:

$$\Delta\nu_{2dc} = [(\tfrac{1}{2}p_0 + q_0)(1 + 2X^{-1} - YX^{-1}) + 2q_0X^{-1}(J - \tfrac{1}{2})(J + 1\tfrac{1}{2})](J + \tfrac{1}{2})$$
$$\Delta\nu_{1dc} = [(\tfrac{1}{2}p_0 + q_0)(-1 + 2X^{-1} - YX^{-1}) + 2q_0X^{-1}(J - \tfrac{1}{2})(J + 1\tfrac{1}{2})](J + \tfrac{1}{2}).$$

Here $Y = A/B_v$, $X = |Y[(Y-4)+(J+\tfrac{1}{2})^2]^{1/2}|$, and p_0 and q_0 are coefficients independent of J which are characteristic of the particular electronic and vibrational state. To determine these constants, the following relations are used:

$$\Delta\nu_{2dc}(J) - \Delta\nu_{1dc}(J) = (p_0 + 2q_0)(J + \tfrac{1}{2})$$
$$\Delta\nu_{2dc}(J) + \Delta\nu_{1dc}(J) = [(p_0+2q_0)(2-Y)(J+\tfrac{1}{2}) + 4q_0(J-\tfrac{1}{2})(J+\tfrac{1}{2})(J+1\tfrac{1}{2})]X^{-1}.$$

The theoretical curves are shown in Fig. 6, for the states $v' = 4$, 5 and 8, drawn according to the p_0 and q_0 values indicated. The agreement is good for $v' = 4$ and 5, but for $v' = 8$ a slight trend in the $\Delta\nu_{1dc}$ points is observed for high J. This is analogous to certain of the results of Mulliken and Christy, and is almost certainly due to the rotational stretching of the molecule.

In the case $v' = 7$, $\Delta\nu_{2dc}$ takes on exceptionally large values, and the experimental points cannot be fitted by curves involving only the two parameters p_0 and q_0. We regard this unusual doubling as having an origin similar to that of the perturbations in $v' = 6$, where quite evidently no simple equations like the above will hold. This will be discussed in the following section.

Perturbations

In the theoretical calculation of Λ-doubling, for a $^2\Pi$ state, certain terms enter which involve a summation over all of the $^2\Sigma$ and $^2\Delta$ states of the molecule. As shown by Mulliken and Christy, however, in many cases the effect is due predominantly to a certain $^2\Sigma$ state, which stands in the relation of "pure precession" to the $^2\Pi$ state and usually contributes a term much greater than the rest. In the present case, judging from the size of the observed p_0 values, this $^2\Sigma$ state is probably a high excited level not yet known experimentally (cf. the analogous case of BO, reference 17, pp. 99, 118). But in the present case a particularly large interaction also occurs for certain values of v and J, in spite of the absence of a relation of pure precession, between the $^2\Pi$ and the lower $^2\Sigma$ ($a^2\Sigma$) states when their rotational levels have nearly the same energy.[27a] According to Kronig[28] this is the cause of the perturbations, or irregularities in the term-series, which have been found in the terms of $a^2\Sigma^{(11)}(J)$ from a study of the CN tail bands.[29] (The superscript in parentheses is used to designate the vibrational quantum number, v). Kronig's theory predicted a corresponding perturbation in the $^2\Pi$ terms for each of those in $a^2\Sigma$. This was partially verified by Rosenthal and Jenkins,[12] who discovered a marked perturbation in the terms near $^2\Pi_{3/2}{}^{(6)}$ ($13\tfrac{1}{2}$), corresponding to that

[27a] Cf. reference 17, expecially pp. 110, 113–4, for a discussion of the relation between Λ-doubling and perturbations.

[28] R. de L. Kronig, Zeits. f. Physik **50**, 347 (1928).

[29] F. A. Jenkins, Phys. Rev. **31**, 539 (1928).

previously known near $a^2\Sigma^{(11)}(13\frac{1}{2})$. For this work, an analysis of the 6,2 band of the red system was made, from the same plates as those used in the present investigation. Rosenthal and Jenkins also showed that the $a^2\Sigma^{(11)}(J)$ terms undergo further perturbations at $J=25\frac{1}{2}$ and $27\frac{1}{2}$.

Since the existence of perturbations depends on the near coincidence of levels of the same J in two different electronic states, it is necessary to find the relative positions of the rotational levels in the two states. If the crossing is to occur at a relatively small value of J, it is obvious that the vibrational levels must also approach each other closely. In Fig. 7a we have drawn to scale the vibrational terms for the four states $a^2\Sigma$, $^2\Pi_{3/2}$, $^2\Pi_{1/2}$ and $b^2\Sigma$. The

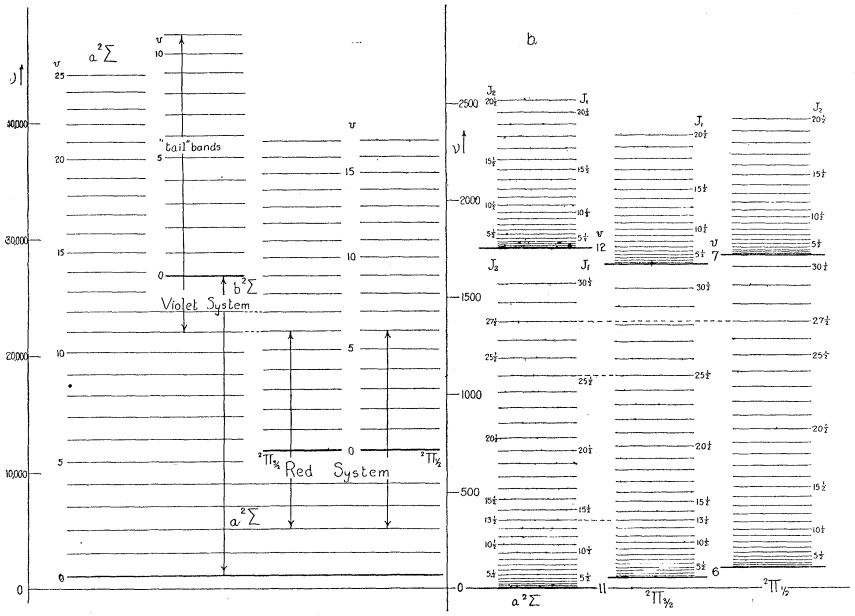

Fig. 7. (*a*) Electronic and vibrational terms of CN. The levels drawn to scale, with the vibrationaless condition of $a^2\Sigma$ as the zero of energy. Transitions are indicated giving one of the strongest bands of the red system, the violet system, and the tail bands, which are part of the violet system.

(*b*) Vibrational levels $a^2\Sigma^{(11)}$, $a^2\Sigma^{(12)}$, $^2\Pi$ $^{(6)}$ and $^2\Pi^{(7)}$ with the associated rotational levels. The scale is magnified $16\frac{2}{3}$ times over *a*, and measured from $a^2\Sigma^{(11)}$ (0) as zero. Displacements of the rotational levels are found at the perturbations (but not shown in the figure), which occur where levels in $a^2\Sigma$ cross those in $^2\Pi$ with the same J value. These points are designated by the horizontal dashed lines.

$^2\Pi$ terms were found from the observed ΔG_v values for the range in which they are available from the red bands, ($\Delta G_{41/2}$ to $\Delta G_{101/2}$) and the remainder extrapolated by the vibrational equation deduced below. The terms for $a^2\Sigma$ and $b_2\Sigma$ are values derived by Birge from a study of the existing data on the violet system, and kindly made available to us in advance of publication. The ΔG_v values of $a^2\Sigma$ are known experimentally only for low v (0 to 3) from the ordinary violet CN bands, and for a range of high v (9 to 15) from the tail bands.

Nevertheless, Birge finds that they both fit a linear $\Delta G_v : v$ curve accurately, and so the absolute magnitudes of the higher G_v terms can be computed with some precision. The numerical values used in Fig. 7a are given in Table V. It will be seen that $a^2\Sigma^{(11)}$ and $a^2\Sigma^{(12)}$ lie very close to $^2\Pi^{(6)}$ and $^2\Pi^{(7)}$ respectively. This accounts for the fact that the only anomalies such as perturbations and unusual Λ-doubling observed in the red system occur in the initial states $v' = 6$ and 7. It accounts equally well for the fact that the only anomalies connected with the *final* state of the tail bands[29] are the perturbations in $v'' = 11$, and the unusually large spin doubling in $v'' = 12$.

To examine the situation in more detail, we consider the relative positions of the rotational levels associated with the above-mentioned vibrational states. These are plotted to scale in Fig. 7b, from the numerical values given in Table V. Since the absolute values of the vibrational terms are not known with great exactness for the $a^2\Sigma$ state in this range of v, their positions relative to $^2\Pi$ are best determined by the perturbations. These show that the terms T_{1c} in $^2\Pi_{3/2}{}^{(6)}$ are crossed by the T_2 terms of $^2\Sigma^{(11)}$ between $J = 12\frac{1}{2}$ and $13\frac{1}{2}$. In the article by Rosenthal and Jenkins,[12] it was assumed from theoretical grounds that the T_{1c} terms could only be perturbed by T_1 terms in the $^2\Sigma$ state. That this is not necessarily true, and that the displacements of the

TABLE V. *Term values of the CN molecule.*
a. Vibrational terms, $G_v + T_e$.

v	$a^2\Sigma$	$^2\Pi_{3/2}$	$^2\Pi_{1/2}$	$b^2\Sigma$
0	1,031.16	11,908.43	11,960.63	28,828.99
1	3,073.55	13,671.32	13,723.52	28,952.49
2	5,089.46	15,408.45	15,460.65	31,035.59
3	7,078.87	17,119.81	17,172.01	33,076.59
4	9,041.80	18,805.40	18,857.61	35,072.69
5	10,978.23	20,465.09	20,517.30	37,030.79
6	12,888.18	22,099.00	22,151.52	38,917.39
			p	
7	14,771.63	23,707.50	23,758.39	40,759.49
8	16,628.60	25,290.10	25,341.75	42,544.59
9	18,549.07	26,846.97	26,898.62	44,270.69
10	20,263.06	28,377.83	28,429.48	45,936.00
11	22,040.55	29,883.09	29,934.74	47,538.76
12	23,791.56	31,362.56	31,414.20	49,081.18
13	25,516.07	32,816.26	32,867.91	50.564.76
14	27,214.10	34,244.19	34,295.84	51,993.04
15	28,885.63	35,646.36	35,698.01	53,369.53
16	30,530.67	37,022.76	37,074.41	
17	32,149.23	38,373.40	38,425.05	
18	33,741.29			
19	35,306.87			
20	36,845.95			
21	38,358.55			
22	39,844.65			
23	41,304.27			
24	42,737.39			
25	44,144.03			

TABLE V. (*Continued*).
*Term values of the CN molecule.**
b. Rotational terms (Smoothed in perturbed regions)

J_1	J_2	$^2\Sigma^{(11)}$	$^2\Pi_{3/2}{}^{(6)}$	$^2\Pi_{1/2}{}^{(6)}$	$^2\Sigma^{(12)}$	$^2\Pi_{1/2}{}^{(7)}$	$^2\Pi_{3/2}{}^{(7)}$	$^2\Sigma^{(12)}(J) - {}^2\Pi_{1/2}{}^{(7)}(J)$
$\frac{1}{2}$		0			1752.51			37.62
$1\frac{1}{2}$	$\frac{1}{2}$	3.39	57.35	108.36	1755.86	1714.89	1665.45	36.10
$2\frac{1}{2}$	$1\frac{1}{2}$	10.19	64.97	113.28	1762.58	1719.76	1673.02	34.70
$3\frac{1}{2}$	$2\frac{1}{2}$	20.39	75.81	121.30	1772.61	1727.88	1683.50	33.39
$4\frac{1}{2}$	$3\frac{1}{2}$	33.97	89.80	132.79	1786.04	1739.22	1697.32	32.22
$5\frac{1}{2}$	$4\frac{1}{2}$	50.90	106.68	147.29	1802.81	1753.82	1713.86	31.22
$6\frac{1}{2}$	$5\frac{1}{2}$	71.26	126.75	165.50	1822.96	1771.59	1733.85	30.25
$7\frac{1}{2}$	$6\frac{1}{2}$	94.97	149.67	186.36	1846.37	1792.71	1756.46	29.63
$8\frac{1}{2}$	$7\frac{1}{2}$	122.09	176.12	211.09	1873.25	1816.74	1782.58	29.25
$9\frac{1}{2}$	$8\frac{1}{2}$	152.55	205.25	238.39	1903.35	1844.00	1811.48	28.71
$10\frac{1}{2}$	$9\frac{1}{2}$	186.40	237.93	269.58	1936.93	1874.64	1843.68	28.52
$11\frac{1}{2}$	$10\frac{1}{2}$	223.65	273.36	303.36	1973.69	1908.41	1878.73	28.43
$12\frac{1}{2}$	$11\frac{1}{2}$	264.31	312.29	340.99	2013.99	1945.26	1917.02	28.67
$13\frac{1}{2}$	$12\frac{1}{2}$	308.33	353.84 *p*	381.04	2057.40	1985.32	1958.18	28.88
$14\frac{1}{2}$	$13\frac{1}{2}$	355.82	399.02	425.17	2104.40	2028.52	2002.68	29.45
$15\frac{1}{2}$	$14\frac{1}{2}$	406.51	446.86	471.70	2154.56	2074.95	2050.01	30.07
$16\frac{1}{2}$	$15\frac{1}{2}$	460.70	498.15	522.27	2208.14	2124.49	2100.65	31.01
$17\frac{1}{2}$	$16\frac{1}{2}$	518.15	552.40	575.13	2264.90	2177.13	2154.11	31.84
$18\frac{1}{2}$	$17\frac{1}{2}$	579.02	609.81	631.95	2324.86	2233.06	2210.93	32.81
$19\frac{1}{2}$	$18\frac{1}{2}$	643.15	670.34	691.04	2388.02	2292.05	2270.51	33.89
$20\frac{1}{2}$	$19\frac{1}{2}$	710.72	733.85	754.37	2454.38	2354.13		34.96
$21\frac{1}{2}$	$20\frac{1}{2}$	781.55	800.58	819.81		2419.42		
$22\frac{1}{2}$	$21\frac{1}{2}$	855.82	870.29	889.55				
$23\frac{1}{2}$	$22\frac{1}{2}$	933.35	943.22	961.29				
$24\frac{1}{2}$	$23\frac{1}{2}$	1014.32	1019.13	1037.33				
$25\frac{1}{2}$	$24\frac{1}{2}$	1098.55	1098.26	1115.37				
$26\frac{1}{2}$	$25\frac{1}{2}$	1186.22	1180.37 *p*	1197.71				
$27\frac{1}{2}$	$26\frac{1}{2}$	1277.15	1265.70	1282.05				
$28\frac{1}{2}$	$27\frac{1}{2}$	1371.52	1354.01	1370.69 *p*				
$29\frac{1}{2}$	$28\frac{1}{2}$	1469.15	1445.54	1461.33				
$30\frac{1}{2}$	$29\frac{1}{2}$	1570.22		1556.27				
$31\frac{1}{2}$	$30\frac{1}{2}$			1653.21				

* *Notes:* For the $^2\Sigma$ terms, both J_1 and J_2 apply. For the $^2\Pi_{3/2}$ terms, J_1 alone applies. For the $^2\Pi_{1/2}$ terms, J_2 alone applies.

levels are more symmetrical if it is the T_2 $^2\Sigma$ terms which are perturbed, has been pointed out by Ittmann[30] in a discussion of these perturbations in CN. This change is definitely required by our other results. In Table V we have taken the crossing to occur about $\frac{2}{3}$ of the way between $J = 12\frac{1}{2}$ and $13\frac{1}{2}$. The positions of the remaining terms were then calculated by summing the experimental values of $\Delta_2 F_d$. This places the lowest level of $^2\Pi_{3/2}{}^{(6)}$ 57.3 cm^{-1} above the lowest level of $^2\Sigma^{(11)}$. This figure is probably correct to within 1 or 2 cm^{-1}, and is substantiated by the fact that the two *vibrational* terms given in Table

[30] G. T. Ittmann, Zeits. f. Physik **71**, 616 (1931). We wish to thank Dr. Ittmann and Prof. H. A. Kramers for sending us the manuscript of this paper.

IV differ by 59.4 cm^{-1}. The agreement is remarkable, considering the long extrapolation used by Birge in calculating the high $^2\Sigma$ vibrational terms.

In the analysis of the 6,2 band, it was found that besides the perturbation mentioned above, which affects the Q_1 and $^OP_{12}$ branches in the neighborhood of $J'=13\frac{1}{2}$, the R_1 and R_2 branches are also perturbed at the highest observed values of J. The displacements in the R_1 branch exceed 1 cm^{-1} beyond $J'=22\frac{1}{2}$ and in the R_2 branch beyond $J'=24\frac{1}{2}$. These perturbations evidently correspond to the very large ones found by Rosenthal and Jenkins in the T_1 terms (revised notation) of $^2\Sigma^{(11)}$ at $J=25\frac{1}{2}$ and in the T_2 terms at $J=27\frac{1}{2}$. They are predicted by Ittmann as due to the crossing of these terms by T_{1d} and T_{2d}, respectively. These perturbations are much more violent than that at $J=13\frac{1}{2}$, a fact which probably accounts for our failure to observe lines in the perturbed branches above $J'=22\frac{1}{2}$ and $24\frac{1}{2}$, respectively. One would expect a very strong interaction of T_{1d} of $^2\Pi$ with T_1 of $^2\Sigma$, since at high values of J we have essentially case (b) spin coupling in both, the spins being parallel to K in both of the two states which perturb each other. Similarly, it should also be strong between T_{2d} and T_2, where the spins are anti-parallel to their K's. In Table V, the terms as far as $J=30\frac{1}{2}$ have been computed by extrapolation beyond $J=20\frac{1}{2}$. Very satisfactory evidence for the above-mentioned coincidences is obtained, as will be seen by reference either to the table, or to Fig. 7b.

The interpretation of the unusually large Λ-doubling in $^2\Pi_{1/2}{}^{(7)}$ and of the corresponding spin doubling in $^2\Sigma^{(12)}$ follows from the relative positions and spacings of the associated rotational levels. The level $^2\Pi_{1/2}{}^{(7)}(\frac{1}{2})$ lies only 37.6 cm^{-1} below the lowest T_1 level, $^2\Sigma^{(12)}(\frac{1}{2})$. Further, the $^2\Pi_1{}'_2{}^{(7)}$ levels start off with a spacing which slightly exceeds that in the $^2\Sigma^{(12)}$ state. Levels of the same J in the two states therefore approach each other at first, and, as is evident from the last column of Table V, reach a minimum separation at about $J=11\frac{1}{2}$. It is known that the interaction of two levels becomes greater as their separation decreases, and we should therefore expect a maximum in the Λ- and spin-doubling at $J=11\frac{1}{2}$. This is in accord with observation; the curve of Λ-doubling for $v'=7$ shown in Fig. 6 has a maximum at about $J=11\frac{1}{2}$, and is remarkably similar in form and magnitude to the spin doubling curve for $^2\Sigma^{(12)}$, which also reaches a maximum at the same J value.[31]

The near equality of the constant B_v in the two perturbing state ($B_v=1.5855$ in $^2\Pi^{(6)}$, 1.6945 in $a\ ^2\Sigma^{(11)}$) is of some importance in permitting the large interactions here observed. The unperturbed rotational levels cross each other gradually in this case, with the result that some come into very close coincidence.

Another important factor in causing the relatively large interaction observed is the fact that the $U(r)$ curve of the $^2\Pi$ state approaches that of the $a\ ^2\Sigma$ state very closely for moderate and large v values. According to Morse curves constructed by one of the writers, the outer branch ($r>r_e$) of the $U(r)$ curves of the $^2\Pi$ state crosses that of the $a\ ^2\Sigma$ state at an almost grazing angle in the neighborhood of $v=14$ of the $^2\Pi$ state. The two curves then remain nearly in coincidence for higher v values. According to this, the observed per-

[31] Fig. 2 of reference 29.

turbations at $v=6$ or 7 come below the crossing point, but the two $U(r)$ curves are already very near together. This is important because it means that the vibrational part of any $^2\Pi$ wave-function has a pronounced maximum at nearly the same value of r as that of any $^2\Sigma$ wave-function which has nearly the same energy. This tends to make the two wave-functions interact strongly.

Although the near approach of the $U(r)$ curves and of certain rotational levels of the $^2\Sigma$ and $^2\Pi$ states favor large interactions and large perturbations, it is probable that in respect to the electronic parts of their wave-functions, these two states are very unfavorable for interaction. Hence as a net result the observed perturbations are not very large.

In the 6,2 band, the Q_1 branch, as recorded in Table I, has two lines representing each of the J' values $12\frac{1}{2}$ and $13\frac{1}{2}$. This duplicity results from the fact that when the states interact very strongly, their wave-functions become "mixed," in such a way that $^2\Pi$ receives some of the characteristics of $a\ ^2\Sigma$, and vice versa. As a result, transitions become possible which have partially the character of transitions from $a\ ^2\Sigma^{(11)}$ to $a\ ^2\Sigma^{(2)}$, and this accounts for the extra lines. In a similar way, extra lines were observed in the tail band $b\ ^2\Sigma^{(11)} \rightarrow a\ ^2\Sigma^{(11)}$, for the same J values. These lines really could equally well be designated $b\ ^2\Sigma^{(11)} \rightarrow {}^2\Pi^{(6)}$. The microphotometer curve of Fig. 2d illustrates the intensity relations near the perturbation in the 6,1 band.

TABLE VI. *Intensities, band heads and band origins.*

v'	$v''=0$	1	2	3	4	5	6	
0	(10,937)							
1	(12,697)	(10,654)						
2	**1** (14,431)	(12,393)						
3	**1** 16,136.57 16,132.43	(14,098)	(12,086)					
4	**2** (17,828)	**6** 15,788.04 15,784.10	(13,772)	(11,782)				$\Delta G'$ 1659.69
5	**1** 19,489.54 19,486.22	**7** 17,447.33 17,443.79	**10** 15,431.55 15,427.75	(13,446)	(11,480)			1634.22
6	**2** (21,121)	**5** 19,081.27 19,078.00	**9** 17,065.46 17,061.98	**7** 15,075.87 15,072.14				1606.87
7		**4** 20,688.02 20,684.92	**6** 18,672.09 18,668.80	**6** 16,682.51 16,679.00	**3** 14,719.39 14,715.61			1583.35
8		**0** 22,271.19 22,268.40	**3** 20,255.07 20,252.13	**5** 18,265.49 18,262.37	**3** 16,302.27 16,298.95	**1** (14,361)		1556.87
9				**1** 19,822.15 19,819.25	**4** 17,858.89 17,855.82	**2** 15,922.08 15,918.81		1530.86
10				**2** 21,352.79 21,350.07	**1** 19,389.55 19,386.68	**1** 17,452.72 17,449.67	**1** (15,540)	1505.26
11				**0** 22,857.87 22,855.29	**1** 20,894.72 20,892.01		**0** (17,041)	
	$\Delta G''$ 2042.43	2016.06	1989.80	1963.38	1937.01			

Vibrational Structure

In addition to the rotational structure of the seven bands given in Table I. we have measured the R_2 head of every band appearing with any intensity, in order to derive equations for the vibrational energy. The results are given in Table VI, the frequency of the head in vacuum being the upper of the two frequencies given for each band. Frequencies given in parentheses are those of bands which were too weak to measure on our plates. The frequencies given are from measurements of Fowler and Shaw, and Asundi and Ryde. They were not used in our analysis, because not very accurate.

Each R_2 head is very near the origin ν_2 of a $^2\Pi_{1/2} \rightarrow {}^2\Sigma$ band. The corrections necessary to convert heads to origins are easily made from our data, as follows. From the term-formulas (3) we find

$$\nu_h - \nu_2 = (\tfrac{1}{4})B_v'' - B^{*2}_{v,-1/2}/4(B^*_{v,-1/2} - B_v'').$$

The origin ν_0 of the complete band is $(\nu_h - \nu_2 - A/2)$ cm^{-1} from the R_2 head. Applying the correction $\nu_h - \nu_2$ to the head frequencies eliminates the rotational energy, and yields the values ν_2, which are also given in Table VI. The combination principle applied to vibrational term differences obtained from our data gives values of ΔG which are consistent to a few hundredths cm^{-1} in all cases where the measurement was reliable. The data for the (3,0), (5,0), (8,1) and (10,3) bands may be somewhat in error, because of the indistinctness of the heads. The R_{21}, R_1, and Q_1 heads were in general more difficult to measure than R_2, and the data are omitted.

The vibrational differences for the lower state fit the equation

$$\Delta G_v'' = 2068.792 - 26.352(v'' + \tfrac{1}{2})$$

with a mean deviation of 0.02 cm^{-1}. This agrees very well with Heurlinger's expression[6] from the violet bands, which gave $\omega_e = 2068.89$, $2x_e\omega_e = 26.50$.[32] The upper state differences are not nearly as regular. In deriving the equation, we were obliged to omit the experimental values of $\Delta G_{61/2}$ and $\Delta G_{71/2}$, as they obviously did not fit in with the others. The equation adopted is

$$\Delta G_v' = 1788.659 - 25.766\,(v' + \tfrac{1}{2})$$

with deviations (obs.-calc.) for $\Delta G_{41/2}$ to $\Delta G_{101/2}$ of -0.13, $+0.16$, -1.35, $+0.82$, $+0.10$, -0.14, $+0.13$ cm^{-1}, in order. It will be noticed that $\Delta G_{61/2}$ is smaller than expected, and $\Delta G_{71/2}$ larger. This would be explained if the vibrational terms of two electronic states in coming close together "repelled" each other, as do rotational states at a perturbation, for then the $^2\Pi^{(6)}$ level would be shifted up, and $^2\Pi^{(7)}$ down (see Fig. 7b). Support for this idea is found in the fact that the interval $\Delta G_{111/2}$ in $a\ ^2\Sigma$, as found from the tail bands,[29] is about 2 cm^{-1} larger than expected, and $\Delta G_{121/2}$ about 0.7 cm^{-1} smaller. That it is somewhat arbitrary to distinguish between a "vibrational" and a "rotational"

[32] As pointed out to us by Professor Birge, this value for $2x_e\omega_e$ was originally given by Heurlinger, misquoted as 27.50 by Kratzer (reference 8), and erroneously copied by Jevons (reference 7) and Birge (reference 9).

perturbation is indicated by the results of Rosenthal and Jenkins.[33] A "vibrational perturbation" occurs when a whole set of rotational levels is simultaneously perturbed. It is true, however, that in these cases one cannot represent all of the band origins by a smooth function. The abnormal values of A determined experimentally for $v'=6$ and 7 (see Table IV) probably are due to the above effect. The best representation of the band origins is, from the above results:

$$\nu_0 = 11{,}043.20 + 1788.66(v' + \tfrac{1}{2}) - 12.883(v' + \tfrac{1}{2})^2 - 2068.79(v'' + \tfrac{1}{2}) + 13.176(v'' + \tfrac{1}{2})^2.$$

The vibrational intensity distribution in this system is shown by the bold face numbers in Table VI, most of which are eye estimates from the work of Fowler and Shaw.[4] We have added the 8,1 and 11,3 bands, which appear faintly on our plates. For many of the infrared bands, intensity estimates are not available. In order to establish the hitherto uncertain vibrational numbering of the $^2\Pi$ states, we have drawn $U(r)$ curves for the $a\ ^2\Sigma$ and the $^2\Pi$ states, with Morse functions, and have determined the nature of the intensity distribution to be expected in the $^2\Pi \rightarrow a\ ^2\Sigma$ bands according to the method of Condon, using the wave mechanics.[34] Comparison with the observed intensities shows excellent agreement when the $U(r)$ curve of the $^2\Pi$ state is drawn corresponding to the v numbering used here, which is that first proposed by Asundi and Ryde.[5] Any other v numbering gives disagreement. These results make it evident that most of the spectrum must lie in the infrared, largely beyond the reach of photography.

[33] J. E. Rosenthal and F. A. Jenkins, Proc. Nat. Acad. Sci. **15,** 896 (1929).
[34] Cf. E. U. Condon, Proc. Nat. Acad. Sci. **13,** 462 (1927), and Phys. Rev. **32,** 858 (1928)

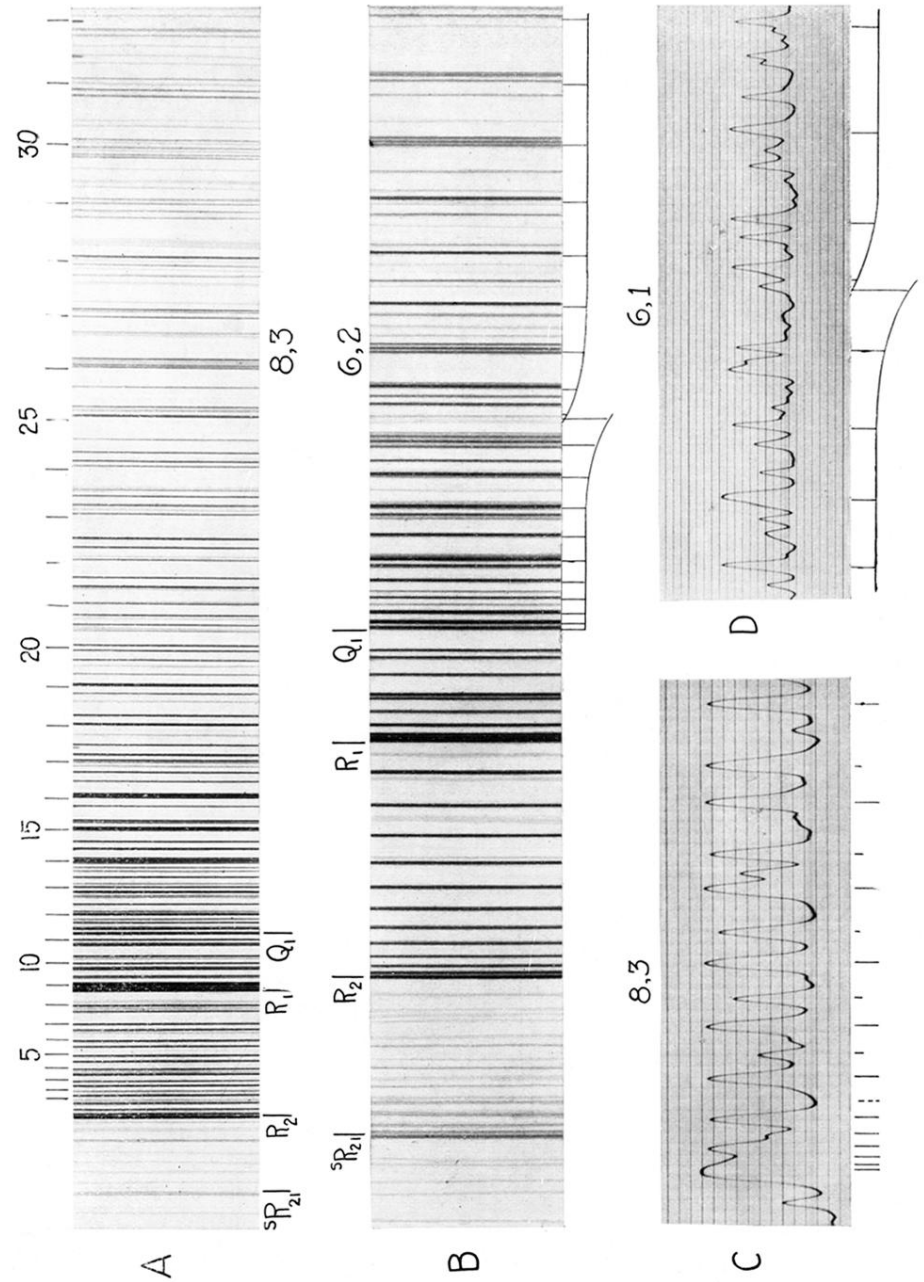

Fig. 2. Bands of the red CN system. *A*. The 8,3 band. The four heads are marked below. Above, the Q_2 lines are designated, and numbered with the values of K''. Wave-lengths increase to the right. *B*. The 6,2 band, enlarged somewhat more than the 8,3 band in *A*. The perturbed branch Q_1 is marked below. Displacements of the lines toward the red or toward the violet are indicated by a rise or fall of the otherwise horizontal connecting line. *C*. Microphotometer curve of the first part of the 8,3 band. The position of the single missing line between the two strong branches R_2 (long lines) and Q_2 (short lines) is indicated by the dotted line. *D*. Microphotometer curve of the main perturbation in the 6,1 band, corresponding to that shown in *B* for the 6,2 band.